Research papers

Carbonate rhizoliths in loess and their implications for paleoenvironmental reconstruction revealed by isotopic composition: $\delta^{13}C$, ^{14}C

M. Gocke [a,*], K. Pustovoytov [b], P. Kühn [c], G.L.B. Wiesenberg [a], M. Löscher [d], Y. Kuzyakov [a]

[a] Department of Agroecosystem Research, BayCEER, University of Bayreuth, 95447 Bayreuth, Germany
[b] Institute of Soil Science and Land Evaluation (310), University of Hohenheim, 70593 Stuttgart, Germany
[c] Institute of Geography, Laboratory of Soil Science and Geoecology, University of Tübingen, 72070 Tübingen, Germany
[d] Max-Reger-Weg 3, 69181 Leimen, Germany

ABSTRACT

Loess–paleosol sequences are important terrestrial archives for studying Quaternary climate changes. They often contain secondary carbonates including e.g. rhizoliths (calcified roots). These secondary carbonates are precipitated in isotopic equilibrium with root-derived CO_2 and are therefore used to reconstruct the vegetation present during their formation based on stable carbon isotopic composition ($\delta^{13}C$). Usually, the chronological context of secondary carbonates in general is not mentioned, because it is assumed that they are formed synsedimentary with loess deposition.
The loess–paleosol sequence at Nussloch, SW Germany, contains in its youngest part (Upper Würmian) large carbonate rhizoliths with diameters of up to 5 cm and lengths of up to 1 m and more, which have not been described in this profile so far. We investigated rhizoliths as well as loess adjacent to and distant from rhizoliths for carbonatic carbon (C_{carb}) and organic carbon (C_{org}) contents, as well as their isotopic composition ($\delta^{13}C$, radiocarbon dating), to identify the rhizolith origin and the time frame of their formation. Considering the ^{13}C fractionation by carbonate precipitation, the $\delta^{13}C_{carb}$ values (-10.9 ± 0.1‰) revealed C_3 plant origin of the rhizolith carbonate and the absence of large amounts of occluded primary loess carbonate. Similar ^{14}C ages of rhizolith C_{carb} and C_{org} (3788 ± 59 years BP and 3150 ± 59 years BP, respectively) argued for the absence of postsegregational alteration. Therefore they are suitable for the reconstruction of paleoenvironmental conditions after loess sedimentation. The ^{14}C ages clearly indicate that rhizoliths did not form synsedimentary. Roots penetrated the loess at Nussloch after the deposition had ceased at ~15 ka BP. Even in the loess adjacent to the rhizoliths (up to a distance of 5 cm), $\delta^{13}C_{carb}$ values indicate the presence of secondary carbonate deriving from postsedimentary organic matter of origin other than that of the reference loess material. Hence, this postsedimentary input of younger root biomass might have masked the initial plant signal in loess–paleosol sequences, which could cause uncertainties for paleoenvironmental reconstructions based solely on loess organic matter.

1. Introduction

Loess–paleosol sequences represent one of the most informative terrestrial paleoclimatic archives (Pye and Sherwin, 1999). A broader application of dating techniques to loess–paleosol sequences, especially optically stimulated luminescence (OSL) method (reviewed by Roberts, 2008; Kadereit et al., 2010), as well as detailed sedimentological (Kemp et al., 1994; Xiao et al., 1995) and paleopedological studies (Mason et al., 2008) contributed to an improved understanding of past climate fingerprints in loess and corresponding terrestrial environments. In those pedosedimentological complexes, secondary carbonate accumulation occurs frequently among the most prominent

pedogenic features. Together with loess dolls, remains of calcified roots are a typical feature of loess–paleosol sequences (Becze-Deák et al., 1997; Kosir, 2004). Cerling (1984) showed for the first time that secondary carbonate in modern soils forms in isotopic equilibrium with soil CO_2, which derives mainly from root respiration and microbial decomposition of soil organic matter (Deines, 1980). Secondary carbonates are therefore used as an important tool for the reconstruction of paleoenvironmental conditions by stable carbon and oxygen isotopic composition ($\delta^{13}C$, $\delta^{18}O$; Quade and Cerling, 1995; Mora et al., 1996; Buck and Monger, 1999; Pustovoytov et al., 2007a), as well as for radiocarbon dating (^{14}C) of soils and paleosols (Amundson et al., 1994; Pustovoytov et al., 2007b). One major prerequisite is that incorporation of older C (e.g. from parent material) and younger C (by postsegregational alteration) can be excluded. In loess deposits, secondary carbonates have been studied by a series of instrumental methods, including micromorphology

(Klappa, 1980; Becze-Deák et al., 1997; Kosir, 2004; Wang et al., 2004; Wang and Greenberg, 2007), stable carbon isotope composition (δ^{13}C; Wang et al., 2000; Pustovoytov and Terhorst, 2004; Wang and Greenberg, 2007; Łącka et al., 2009) and radiocarbon dating (Pustovoytov and Terhorst, 2004; Asano et al., 2007).

Most studies based on carbon isotopic composition (δ^{13}C, ^{14}C) of secondary carbonates were performed on carbonate coatings on clasts (Amundson et al., 1989; Monger et al., 1998; Pustovoytov et al., 2007a, b) and small secondary carbonate concretions including soft powdery lime, pseudomycel or small nodules (Buck and Monger, 1999; Khokhlova et al., 2001). Becze-Deák et al. (1997) recognized the high potential of calcified roots for chronological and paleoenvironmental studies due to their formation in rather short periods. For instance, Jaillard (1992) observed that crystals of calcified root cells can form within 24 h. Calcified roots are termed in literature under different names: beinbrech, osteokollen (Greek osteon = bone, Latin collon = stem; Ziehen, 1980), rhizomorphs, rhizo(con)cretions, root casts, pedotubules, and rhizoliths (summarized by Klappa, 1980) from which we chose the term 'rhizolith'. Rhizoliths are formed by encrustation of plant roots by secondary carbonate (Klappa, 1980; Jaillard et al., 1991; Becze-Deák et al., 1997). They occur, sometimes with a high amount of gypsum (Dultz and Kühn, 2005), in sandy and silty calcareous sediments (Ziehen, 1980; Becze-Deák et al., 1997; Cramer and Hawkins, 2009).

Although calcified root cells and small rhizoliths were used for several studies as a tool for reconstructing paleoenvironmental conditions (Wang et al., 2000; 2004) and paleovegetation (Wang and Greenberg, 2007), the chronological context of these calcified roots was never determined by radiocarbon dating in these studies. Instead, the authors linked the age of the rhizoliths to the age of surrounding loess or paleosol organic matter (OM). However, as shown by Pustovoytov and Terhorst (2004) for calcified root cells from SW Germany, the ages of loess and secondary carbonate nodules may not necessarily be the same, rather the secondary carbonates may have formed after loess sedimentation by encrustation of plant roots penetrating the loess–paleosol sequence after sedimentation. Therefore, the abovementioned studies based on stable carbon isotopic composition of secondary carbonate in loess–paleosol sequences should be regarded with caution. Two further factors complicate the correct interpretation of paleoenvironmental and chronological information within secondary carbonates as e.g. rhizoliths: On the one hand, incorporation of older carbonate, e.g. from parent material into the secondary carbonates might entail an overestimation of ^{14}C ages. On the other hand, postsegregational alteration of the secondary carbonate, introducing younger atmospheric CO_2, can distort the chronological information used for radiocarbon dating and lead to an underestimation of radiocarbon ages of secondary carbonate (Chen and Polach, 1986; Amundson et al., 1994; Budd et al., 2002).

Most studies about secondary carbonates in loess–paleosol sequences focused on relatively small-sized calcified roots (some 0.5–2 mm in diameter and 5–20 mm in length). Beyond this morphological variety, there are also relatively large, solid calcified roots (diameter up to 5 cm, length up to 1 m and more), which, however, occur less frequently in loess–paleosol sequences (Ziehen, 1980) and were mentioned in SW Germany only from calcareous dune sands (Löscher and Haag, 1989). Presumably, such large rhizoliths are suitable to improve our knowledge about the chronological context of this special form of secondary carbonate and the potential contamination with older or modern carbon. Therefore, we investigated large calcified roots obtained from the late Quaternary loess–paleosol sequence at Nussloch (SW Germany) to elucidate their potential for paleoenvironmental research and loess chronostratigraphy.

Better understanding of the origin and formation of rhizoliths in loess–paleosol sequences, and thus of carbonate dynamics in calcareous sediments in general, can help to improve interpretations of paleoenvironmental and chronological data in loess–paleosol sequences. For our study, we chose rhizoliths from Nussloch, SW Germany, because this loess–paleosol sequence is properly investigated (Rousseau et al., 2007; Antoine et al., 2009) and provides a well developed Weichselian loess interval of up to 18.5 m thickness (Antoine et al., 2001). The rhizoliths are well accessible in a fresh section without alteration by modern pedological processes. We wanted to determine the portions of primary and secondary carbonate in rhizoliths and loess, as well as potential incorporation of OM from former root biomass in loess distant to rhizoliths. Therefore, we analyzed C_{carb} and C_{org} contents and their isotopic composition in microtransects through rhizoliths (from the center to the outer parts) as well as in macrotransects from rhizoliths via rhizosphere loess towards reference loess, which was obtained from the same depth as rhizoliths, but at a distance of 50–70 cm from rhizoliths. Micromorphological investigation of rhizoliths was used to support and improve understanding of results from carbon (C) analyses. The aim of this first study on inorganic and organic C in rhizoliths and surrounding materials was to prove their relevance for paleoenvironmental studies of terrestrial sedimentary sequences.

2. Methods

2.1. Study site

The study site is located near Nussloch, SW Germany, on the eastern side of the Rhine Rift Valley, about 10 km south of Heidelberg. Loess and rhizoliths were sampled at the open cast mine of HeidelbergCement AG (49.19°N, 8.43°E, 217 m a.s.l.). The loess–paleosol sequence with a total thickness of 18.5 m was formed during the last glacial–interglacial cycle (Zöller et al., 1988; Hatté et al., 1998) and shows the climatic record of the last 130 ka (Hatté et al., 1999). A detailed description of the Nussloch sequence is provided by Antoine et al. (2001).

Contrary to previous descriptions of the Nussloch loess profile (Antoine et al., 2001, 2009), rhizoliths with irregular shape and size occur in a recently prepared section nearby (~100 m) the standard profile P4 (Antoine et al., 2001) from 1 m below the present surface down to a depth of at least 8 m. The rhizoliths reach sizes of up to 5 cm in diameter (Fig. 1) and can be traced over depth intervals of several dm up to ca. 1.5 m. In contrast to rhizoliths, large loess dolls, the formation of which does not occur in close spatial relation to roots, occur from 6 m downwards.

2.2. Sampling

The sampled section is a new part of the quarry of the HeidelbergCement AG, which was cut two years before the sampling for this study in October 2009. Prior to sampling, the section was cleaned by removing at least 0.5 m of loess with spades. Würmian typical loess was sampled from a depth of 15 m below present surface (in the following named 'reference loess 1') to ensure that the loess is completely primary and not affected by current soil forming processes, i.e. recrystallization of loess carbonate or input and decomposition of fresh plant biomass. Rhizoliths of different shape and diameter were sampled from a depth interval between 1 m and 3 m below present surface. Correlation with the standard profile P4, described by Antoine et al. (2009), ensured that no paleosols were sampled. Due to limited amounts of available material for each rhizolith (especially for $\delta^{13}C_{org}$ determinations and studies of internal transects), different analyses (see below) were performed on different rhizolith samples. As the rhizoliths were most abundant between 1 m and 3 m and reached lengths of more than 1 m, differences related to sampling depth were not relevant.

For two rhizoliths from a depth between 2.2 m and 2.6 m below present surface, surrounding loess was sampled in macrotransects from the surface of the rhizolith up to a distance of 2.5 cm (± 0.5 cm; 'rhizosphere loess 1'), and 2.5–5 cm (± 0.5 cm; 'rhizosphere loess 2').
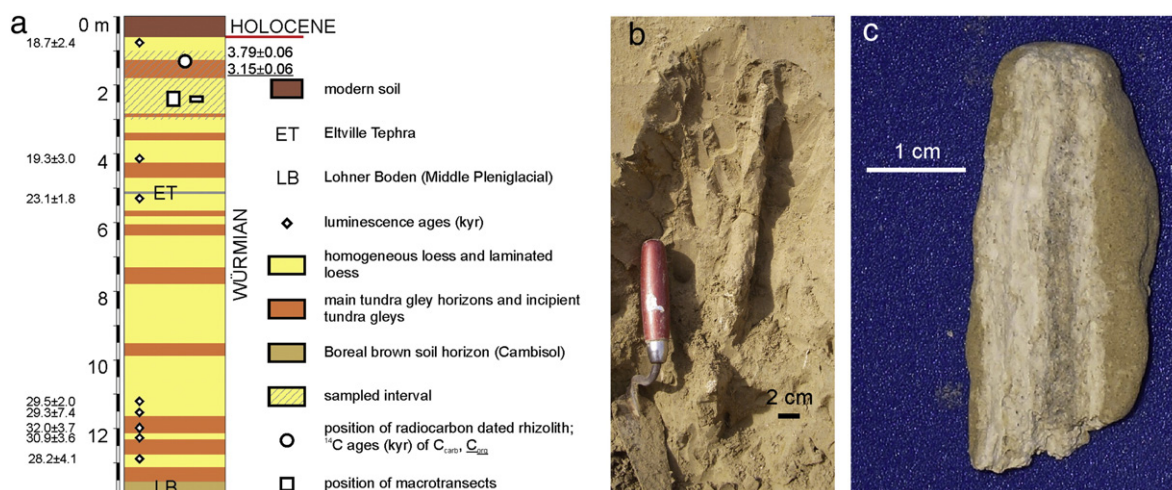
Fig. 1. (a) Stratigraphical chart of the Würmian Upper Pleniglacial loess sequence at Nussloch, modified after Antoine et al. (2009). For luminescence data see Antoine et al. (2009) and references therein. (b) Rhizolith *in situ*. (c) Longitudinal cut through a rhizolith.

Therefore, rhizoliths with adhering loess material were collected and the latter was peeled off using a knife. One typical loess sample without visible root remains was taken from the same depth like these rhizoliths in a distance of 50–70 cm from rhizoliths (in the following named 'reference loess 2'). This sample set refers to Rhizolith 1 and Rhizolith 2 in Fig. 3. Sizes of the samples depended on the sample type and, in case of rhizoliths, on diameter and length: Amounts were 20–100 g for individual rhizolith samples, >50 g for rhizosphere loess samples, and >300 g for reference loess samples. Note that reference loess 2, covering a depth of 40 cm, encompasses sediment accumulated during several thousand years and thus possibly represents a mixture regarding e.g. OM composition and further properties. However, the aim of this study was the comparison of rhizolith-derived OM with synsedimentary loess OM in general and not related to individual stratigraphic units within the profile.

After sampling, all materials were immediately oven-dried at 60 °C until constant weight. Thereafter, loess and several rhizolith samples were ground in a ball mill (MM200, Retsch, Germany), homogenized by combining followed by stirring of the milled aliquots, and stored dry until analyses.

From a depth between 1 and 3 m, three rhizoliths with diameters of 7, 11 and 16 mm (Rhizoliths 3–5 in Fig. 5) were cut longitudinally and carbonate material was abraded by a scalpel in several *microtransects*, each of these with 4–5 distinct samples from the middle of the carbonatic tube to its outer boundary (Fig. 1c). Carbonate material of the microtransects was used for $\delta^{13}C_{carb}$ analyses.

Additionally, one loess doll was sampled at a depth of 6 m for comparison with rhizoliths.

2.3. Micromorphology

Four air dried rhizoliths were impregnated with Oldopal P80-21, cut and polished to 4.8 cm·2.8 cm slices following the procedure of Beckmann (1997). Thin sections were described under a polarizing microscope (Zeiss Imager.A2; Software AxioVision 4.7.2) mainly using the terminology of Stoops (2003). Oblique incident light (OIL) was obtained by an external light source with a double-arm swan neckglass fiber light guide.

2.4. Elemental analyses

Total C_{carb} content of the rhizoliths was determined gravimetrically from ten samples which were taken from depths of 1.1 m, 1.3 m, and between 1.5 and 2 m. The washed and dried (60 °C) samples were crushed, weighed, and reacted with 1 M HCl in excess to remove CaCO3,

subsequently with few drops of 3 M HCl to remove less soluble carbonates like dolomite, and the residuum was subsequently weighed again. Two further rhizoliths and reference loess samples were analyzed for C_{org} and C_{carb} contents by combustion in an oven (Feststoffmodul 1300, AnalytikJena, Germany) connected to an N/C analyzer (Multi N/C 2100, AnalytikJena, Germany). C_{org} contents were determined at 550 °C, while C_{carb} contents were measured at 1000 °C after removing organic matter at 550 °C for 10 min in presence of oxygen. Results of elemental analyses are expressed in mg g^{-1}, with a relative precision of 1%.

2.5. $\delta^{13}C$ analysis

$\delta^{13}C$ analysis was performed on loess C_{carb} (6 samples) and loess C_{org} (5 samples), as well as on secondary carbonate and OM of the rhizoliths. In total, 25 microtransect samples and two bulk rhizolith samples were analyzed for $\delta^{13}C_{carb}$. Few of the rhizolith samples contained remains of ancient root biomass, presumably deriving from shrub or tree vegetation (Gocke et al., 2010a). $\delta^{13}C_{org}$ of rhizoliths was measured in 4 samples.

For $\delta^{13}C_{carb}$ analysis of loess or rhizoliths, aliquots of the samples were heated for 1 h in a muffle furnace at 550 °C to remove organic matter. For $\delta^{13}C_{org}$ analysis, aliquots of the samples were treated with 1 M HCl to remove CaCO_3, subsequently with few drops of 3 M HCl to remove less soluble carbonates like dolomite, and finally washed with de-ionized water. After adding water and shaking the samples, the solid material was sedimented by centrifugation and the supernatant was subsequently removed. After neutralization, samples were dried in an oven at 40 °C.

Stable carbon isotope analyses were performed at the Department of Food Chemistry, University of Hohenheim, Germany on a Delta Plus XL isotope ratio mass spectrometer (Thermo Finnigan MAT, Bremen, Germany) connected to an elemental analyzer EA 3000 (Hekatech, Wegberg, Germany). Results are given in ‰ calculated against V-PDB standard, with an absolute precision of ~0.5‰.

2.6. Calculation of secondary carbonate portions

Using $\delta^{13}C_{carb}$ values of the rhizolith and of loess parent material, the percentage of the carbon fraction originating from root and rhizomicrobial respiration (=portion of secondary carbonate) was calculated as follows (Nordt et al., 1998):

$$\% \text{ secondary carbonate} = \frac{\delta^{13}C_{rhizolithC_{carb}} - \delta^{13}C_{parentC_{carb}}}{\delta^{13}C_{secondaryC_{carb}} - \delta^{13}C_{parentC_{carb}}} \cdot 100 \qquad (1)$$

where $\delta^{13}C_{rhizolithC_{carb}}$ and $\delta^{13}C_{parentC_{carb}}$ are the isotopic signatures of the rhizolith carbonate and the primary loess carbonate (from reference loess 2). $\delta^{13}C_{secondaryC_{carb}}$ is the isotopic signature of pure secondary carbonate (Nordt et al., 1996):

$$\delta^{13}C_{secondaryC_{carb}} = \delta^{13}C_{vegetation} + \varepsilon + v \quad (2)$$

where $\delta^{13}C_{vegetation}$ is the isotopic signature of the plant biomass leading to the formation of the secondary carbonate, ε is temperature dependant isotopic fractionation by carbonate equilibrium reactions (Romanek et al., 1992), and $v = 4.4‰$ is the isotopic fractionation by molecular diffusion of CO_2 (O'Leary, 1981; Nordt et al., 1998). Assuming an average value for ε of 10.5‰, this results in secondary carbonate $\delta^{13}C$ signatures which are ~14.9‰ higher than those of the corresponding plant biomass.

Portions of secondary carbonate were calculated in the same way for the two macrotransect sample sets.

Assuming an absolute analytical precision of 0.5‰ for $\delta^{13}C$ measurement (see above), Gaussian error propagation leads to uncertainty of 8.2% for calculated secondary carbonate portions.

2.7. Radiocarbon dating

One rhizolith from a depth of 1.3 m below present surface was chosen for radiocarbon dating. The age of OM in reference loess was not determined as luminescence data for the Nussloch section are available from literature: Loess accumulation in this region ceased at 15 ka before present (Antoine et al., 2001). The loess surrounding the above mentioned rhizolith has an age of at least 17 ka, but is younger than 20 ka (age of the Eltville Tephra; Fig. 1a; Antoine et al., 2001).

^{14}C ages were determined for bulk rhizolith C_{carb} and in connected former root C_{org} by the AMS facility at the Ångstrom Laboratory of the University of Uppsala, Sweden. For carbonate analysis, the sample was reacted with 0.5 M HCl to release CO_2 from $CaCO_3$. CO_2 was graphitized using a Fe-catalyzed reaction prior to accelerator measurement. To analyze the rhizolith OM, the sample was first heated with 1% HCl and kept for 8–10 h just below the boiling point to remove the carbonate. Afterwards, the sample was heated with 1% NaOH and kept for 8–10 h just below the boiling point to receive the insoluble fraction of OM. This fraction was washed, dried, combusted to CO_2 and graphitized by a Fe-catalyst reaction.

The measured ^{14}C ages were converted to the Calendric Age BP using the online version of CalPal (www.calpal-online.de; quick-cal2007 ver.1.5; Weninger et al., 2007) and reported at the 1σ range and as mean value ± 1σ.

2.8. Calculations and statistics

For triplicate analyses mean values and standard errors of the mean are presented. Especially for rhizolith microtransects the material was not always available for triplicate measurements. Here, mean values and 95% confidence intervals of the mean values were calculated using Prism 5 software (GraphPad Software). All individual results can be assessed in the electronic supplement.

Data sets were tested for significance of differences using one-way ANOVA with a significance level of 0.05, followed by post hoc Scheffé test. These statistical evaluations were performed using STATISTICA 7.0 software (Statsoft).

3. Results

3.1. Micromorphology of rhizoliths

Matrix of the rhizolith carbonate occurs in all thin sections with an open porphyric c/f related structure. Micromass is mainly built up by micritic carbonate and coarse material by sparitic carbonate. Other minerals like quartz, feldspars, and micas, which are attributed to primary loess material, occur only close to the outer boundary areas of the rhizoliths (Fig. 2a, d). A cloudy to circular striated appearance (in OIL) of the micromass shows heterogeneous parts. Cross sections show at least one channel (diameter around 1000 μm) in the central part of the rhizoliths (Fig. 2a–d). As can be seen in longitudinal sections (Fig. 1c), this channel represents the former central cylinder of the root. In three rhizoliths (Fig. 2a–c) more than one center of higher porosity is detectable. Some of the channels have incomplete to complete sparite fillings, which are well expressed as whitish to grayish patches in Fig. 2a and c or loose crumbly incomplete fillings (Fig. 2a–c, e). Rhizolith carbonate consisted mainly of micrite, whereas sparitic channel fillings in all rhizoliths, as well as needle fiber calcite that occurs in one rhizolith (Fig. 2f; Stoops, 1976) indicate the presence of postsegregationally recrystallized carbonate within rhizoliths.

3.2. C_{org} und C_{carb} contents of rhizoliths and loess

According to Bente and Löscher (1987), the Nussloch loess–paleosol sequence shows average C_{carb} contents of 30 mg g^{-1} in loess and 36 mg g^{-1} in the Upper Würmian tundra gleys ('Nassböden'), corresponding to $CaCO_3$ contents of 25% and 30%, whereas C_{org} contents in general are <5 mg g^{-1}.

Reference loess 1 contained 35 mg C_{carb} g^{-1} (29% $CaCO_3$), while it was 46 mg g^{-1} for reference loess 2 (38% $CaCO_3$). These rather high carbonate contents are in accordance with previously reported data from Nussloch (Hatté et al., 1998). The C_{carb} content of the rhizoliths varied between 88 and 116 mg g^{-1} (74–97% $CaCO_3$) and averaged at 102 ± 3 mg g^{-1} corresponding to 85 ± 2% $CaCO_3$ (Fig. 3a). Variations of C_{carb} contents between rhizoliths of different depth were minor and not significant. This average rhizolith C_{carb} content is considerably higher than that of a loess doll (80 mg g^{-1}) from the same profile sampled at a depth of 3.5 m. C_{carb} contents of rhizoliths were significantly ($p<0.01$) higher than those of all loess samples (rhizoloess and reference loess).

C_{org} content was 0.3 mg g^{-1} for reference loess 1 (Wiesenberg et al., 2010) and 8.3 mg g^{-1} for reference loess 2. Rhizoliths showed considerably higher C_{org} contents which differed between the samples depending on the amount of root residues. For two samples from depths between 2.2 m and 2.6 m, the C_{org} content was 54.2 mg g^{-1} and 88.9 mg g^{-1} (Gocke et al., 2010a). C_{org} contents of rhizoliths were significantly ($p<0.05$) higher than those of rhizoloess and reference loess.

C_{carb} and C_{org} contents of rhizosphere loess samples were similar to those values of reference loess 2, sampled at the same depth (Fig. 3a).

3.3. Stable carbon isotopic composition ($\delta^{13}C$)

$\delta^{13}C$ analyses yielded significantly ($p<0.01$) different results for rhizolith C_{org} and for C_{carb} in rhizoliths, reference loess 1 and reference loess 2 (Fig. 4). The carbon isotopic signature of rhizolith C_{org} was −25.9 ± 0.5‰. Minimum and maximum $\delta^{13}C$ values of rhizolith C_{carb} were −12.0‰ and −10.1‰, with an average of −10.9 ± 0.1‰. The isotopic signature of primary loess C_{carb} from a depth of 15 m below present surface (reference loess 1) was −1.2 ± 0.1‰, whereas it was −2.4 ± 0.1‰ for root-free loess in a depth of 2.2–2.6 m (reference loess 2; Fig. 4). The latter value is in agreement with literature data from uppermost Würmian loess in the region south of Heidelberg (Pustovoytov and Terhorst, 2004).

Within the *macrotransects*, $\delta^{13}C_{carb}$ values in rhizoliths were around −11‰ and showed increasing values towards rhizosphere loess as well as from rhizosphere loess towards reference loess 2. $\delta^{13}C_{carb}$ values were significantly different from each other ($p<0.05$) except for rhizoloess 2, which was not different from rhizoloess 1 and
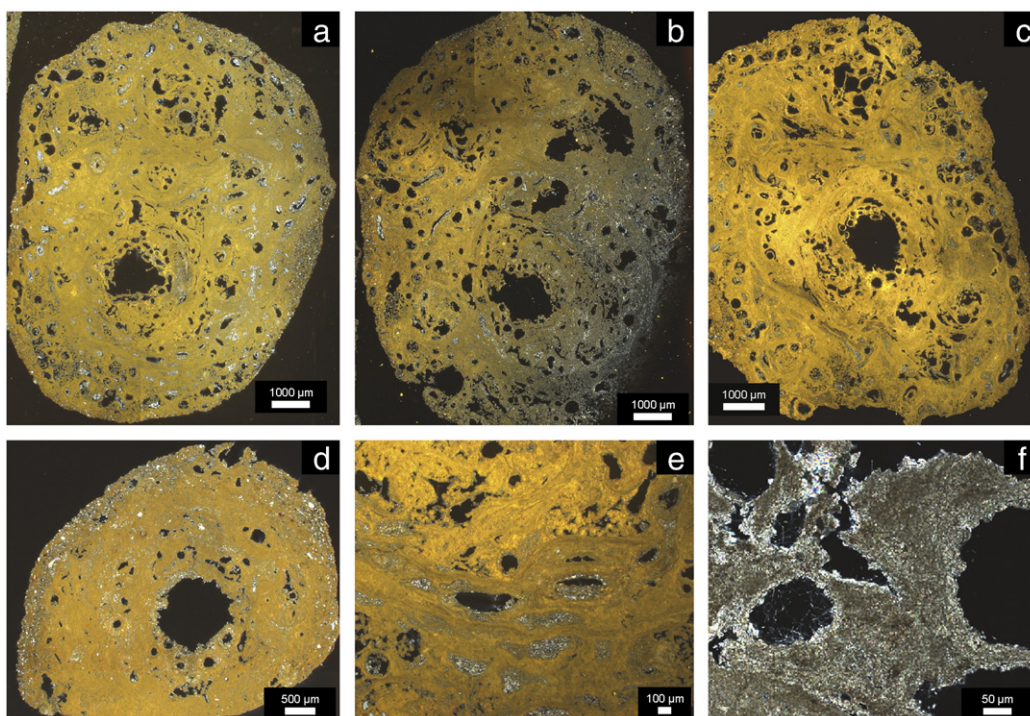
Fig. 2. Cross sections of four different rhizoliths with combined oblique incident light (OIL) and crossed polarizers (XPL); in OIL micrite appears yellowish. (a) Whitish patches are sparite infillings; five centers of higher porosity are visible; total porosity is 20%. (b) Four to five centers of higher porosity are visible; total porosity is 30%. (c) Three centers of higher porosity are visible; whitish patches are sparite infillings; total porosity is 25%. (d) One central channel is surrounded by circular arranged smaller channels (diameter 50–100 μm), total porosity is 15%. (e) Magnification of (a), OIL + XPL: complete and incomplete sparite infillings, loose incomplete crumby infillings (lower left and right hand side), note the cloudy appearance of the micromass and the brighter colors of the more central parts of the rhizolith. (f) Magnification of (c), XPL: needle fiber calcite in channels.

reference loess 2. $\delta^{13}C_{org}$ values within the macrotransects did not show any clear trend. They varied between −24.7 and −25.8‰ without significant differences (Fig. 3b).

$\delta^{13}C_{carb}$ *microtransects* of the smallest (rhizolith 3) and the medium size (rhizolith 4) rhizolith samples showed slightly increasing values from the center to the margin of the tube from −11.2 to −10.6‰ and from −11.1 to −10.6‰, respectively. For the rhizolith sample with the largest diameter (rhizolith 5), the microtransects showed scattering $\delta^{13}C_{carb}$ values around −10.9‰ with no trend of increasing or decreasing values from the center to the margin of the tube (Fig. 5a).

3.4. Portions of secondary carbonate

Using the stable carbon isotopic signatures of primary loess CaCO$_3$ sampled in the same depth as rhizoliths (−2.4‰), rhizolith carbonate and the $\delta^{13}C_{vegetation}$ (−25.9‰) of root residues in the rhizoliths, portions of secondary carbonate, i.e. carbonate with C originating from root-derived CO$_2$, were calculated according to Eq. 1.

Portions of secondary carbonate were high in rhizoliths (microtransects: 91.4–112.5%; Fig. 5b) and decreased to values below 12% in loess adjacent to rhizoliths (rhizosphere loess 1; Fig. 3c). Reference loess was presumed to contain no secondary carbonate (Fig. 3c). The portion of enclosed primary loess carbonate in rhizolith carbonate averaged 1.9 ± 1.1% in all rhizoliths. Here it is important to mention, that this is the calculated contribution of primary carbonates to the rhizoliths based on their $\delta^{13}C$ values. However, as the sensitivity of this approach based on ^{13}C natural abundance is less than 5%, we conclude that nearly no primary carbonates were present in rhizoliths and the recrystallization of carbonate was close to 100%. Therefore, it is correct to apply radiocarbon dating to estimate the age of the rhizoliths.

3.5. Radiocarbon (^{14}C) ages

The calibrated ^{14}C age of the root OM (rhizolith C$_{org}$) recovered from the inner part of the rhizoliths was 3150 ± 59 years. The rhizolith carbonate revealed a slightly higher radiocarbon age of 3788 ± 59 years (Table 1). Hence, carbonate was approximately 640 years older than C$_{org}$ of the same rhizolith.

4. Discussion

4.1. Stable carbon isotopic composition

The difference between $\delta^{13}C$ values of rhizolith C$_{org}$ and rhizolith C$_{carb}$ averaged at 15.0‰ (Fig. 4), thereby strongly suggesting root-derived CO$_2$ as the main or sole source of the rhizolith C$_{carb}$ (Cerling, 1984). $\delta^{13}C$ values of rhizolith C$_{carb}$ further indicate C$_3$ plants as source vegetation of the calcified roots (Nordt et al., 1996) and almost no incorporation of carbonate originating from loess (Alonso-Zarza, 1999; Łącka et al., 2009), which is typically characterized by higher $\delta^{13}C$ values.

Rhizolith $\delta^{13}C_{org}$ values (−25.9 ± 0.5‰) were slightly lower than those of loess C$_{org}$ in the Nussloch loess section ranging mainly between −25 and −24‰ (Hatté et al., 1999). Both rhizolith and loess OM derive from C$_3$ vegetation. In contrast, Pustovoytov and Terhorst (2004) reported higher loess $\delta^{13}C_{org}$ values of up to −16.7‰ from the section of Schatthausen, which is situated in a distance of <1 km of the Nussloch section. The authors discuss the possibility of locally occurring C$_4$ plants, leading to these $\delta^{13}C_{org}$ values, while the Nussloch section does not support this occurrence. Additional explanations for higher $\delta^{13}C_{org}$ values at Schatthausen could be incomplete removal of carbonate or contamination of loess by C from different sources like Sahara dust. Moreover, it is still problematic to correlate both profiles chronostratigraphically due to the greda structure of loess deposits in
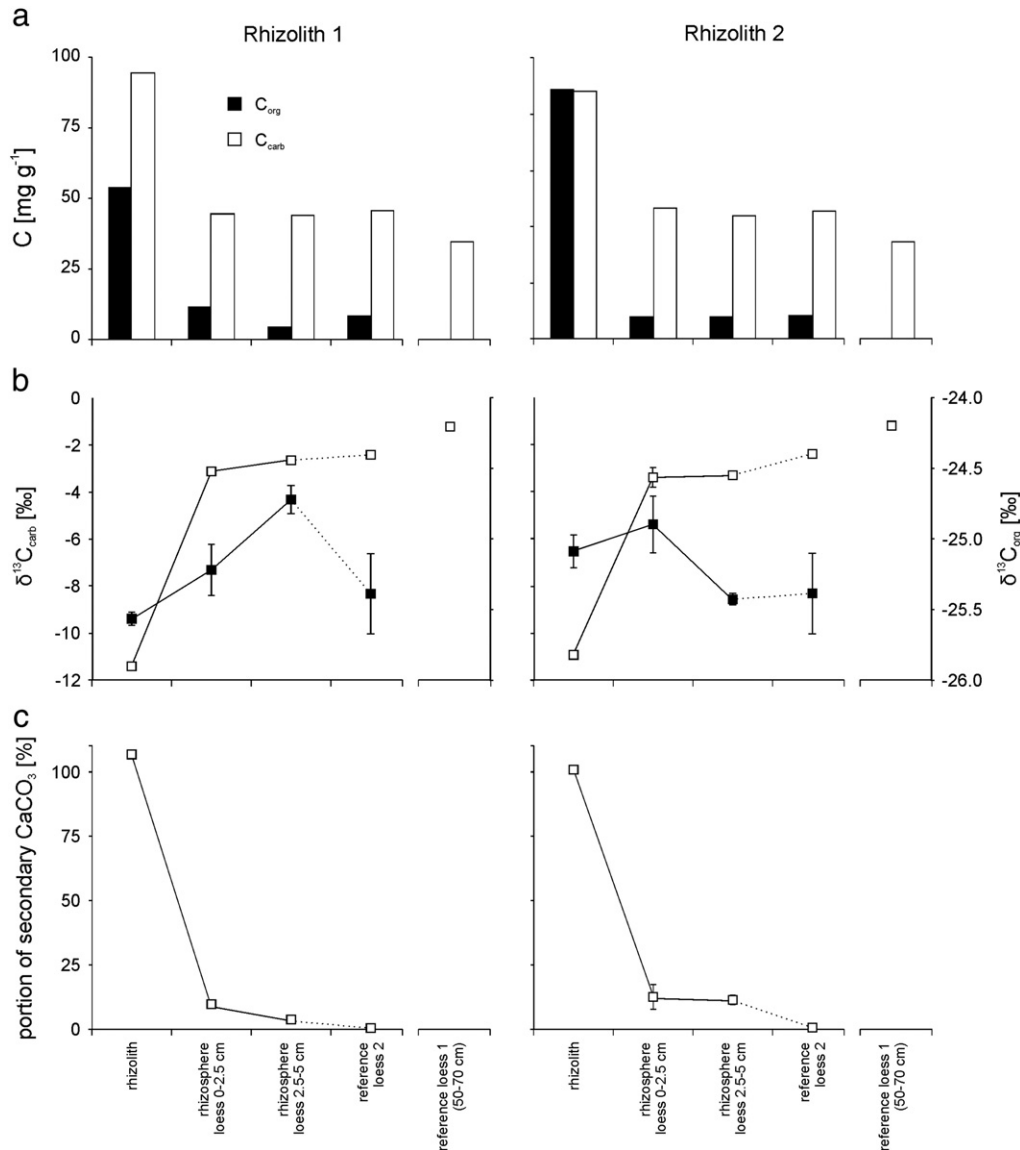
Fig. 3. Macrotransects of two rhizolith samples from a depth of 2.2–2.6 m comprising the rhizolith itself, loess adjacent to the rhizolith and reference loess 2, sampled at a distance of 50–70 cm from rhizoliths. For comparison, results from reference loess 1 (depth 15 m) are also shown. (a) C_{org} and C_{carb} ($CaCO_3$) contents, (b) $\delta^{13}C$ values of C_{org} and C_{carb}, and (c) portions of secondary carbonate in rhizolith and loess, assuming a $\delta^{13}C$ difference between $\delta^{13}C_{vegetation}$ and $\delta^{13}C_{pedogenicCaCO_3}$ of 14.9‰. Error bars (partly smaller than symbol size) show standard error of the mean (SEM) between replicate measurements.

this region, which might have led to differences of the vegetation within short distances.

Portions of secondary carbonate decreased in smaller rhizoliths from the center towards their outer boundary (rhizolith 3 and 4; Fig. 5). This is in agreement with the fact that a high pCO_2 related to root and rhizomicrobial respiration is maintained only at the root surface and decreases within few millimeters distance (Hinsinger et al., 2003). Moreover, primary mineral grains, i.e. also primary loess carbonate with higher $\delta^{13}C_{carb}$ values, occur mainly in the outer parts of the rhizoliths (Fig. 2a, d). A trend of decreasing portions of sec-
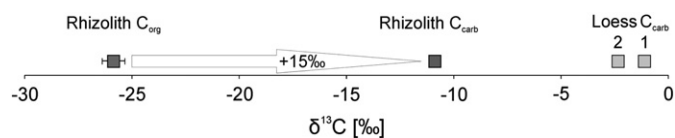

Fig. 4. Average $\delta^{13}C_{carb}$ values from loess (reference loess 1 from 15 m below present surface, reference loess 2 from 2.2 to 2.6 m below present surface) and rhizoliths and $\delta^{13}C_{org}$ values from rhizoliths. Error bars (partly smaller than symbol size) show SEM between real replicates.

ondary carbonate from the center towards outer parts was, however, not visible in the rhizolith with the largest diameter (rhizolith 5). On the contrary, values in this rhizolith strongly varied and showed a broad spectrum of secondary carbonate portions between 91.4 and 112.5% (Fig. 5). As shown by micromorphology, these fluctuations may be caused by the influence of smaller roots adjacent to the main root which were either not calcified or calcified and 'incorporated' into the main rhizolith (see smaller channels in Fig. 2a–c). In general, high secondary carbonate portions in rhizoliths (≫90%) indicate that almost complete isotopic exchange occurred during rhizolith forma-tion by dissolution of primary loess $CaCO_3$ and reprecipitation of carbonate with CO_2 produced by root and rhizomicrobial respiration.

4.2. Radiocarbon ages and rhizolith conservation

The ^{14}C ages of rhizolith C_{org} (3150 years) and C_{carb} (3790 years) revealed Holocene formation of the rhizolith, in contrast to a late Pleistocene age of surrounding loess (17–20 ka; Antoine et al., 2001).

Contrary to carbonate coatings used for determination of the time frame of secondary carbonate formation by radiocarbon dating of
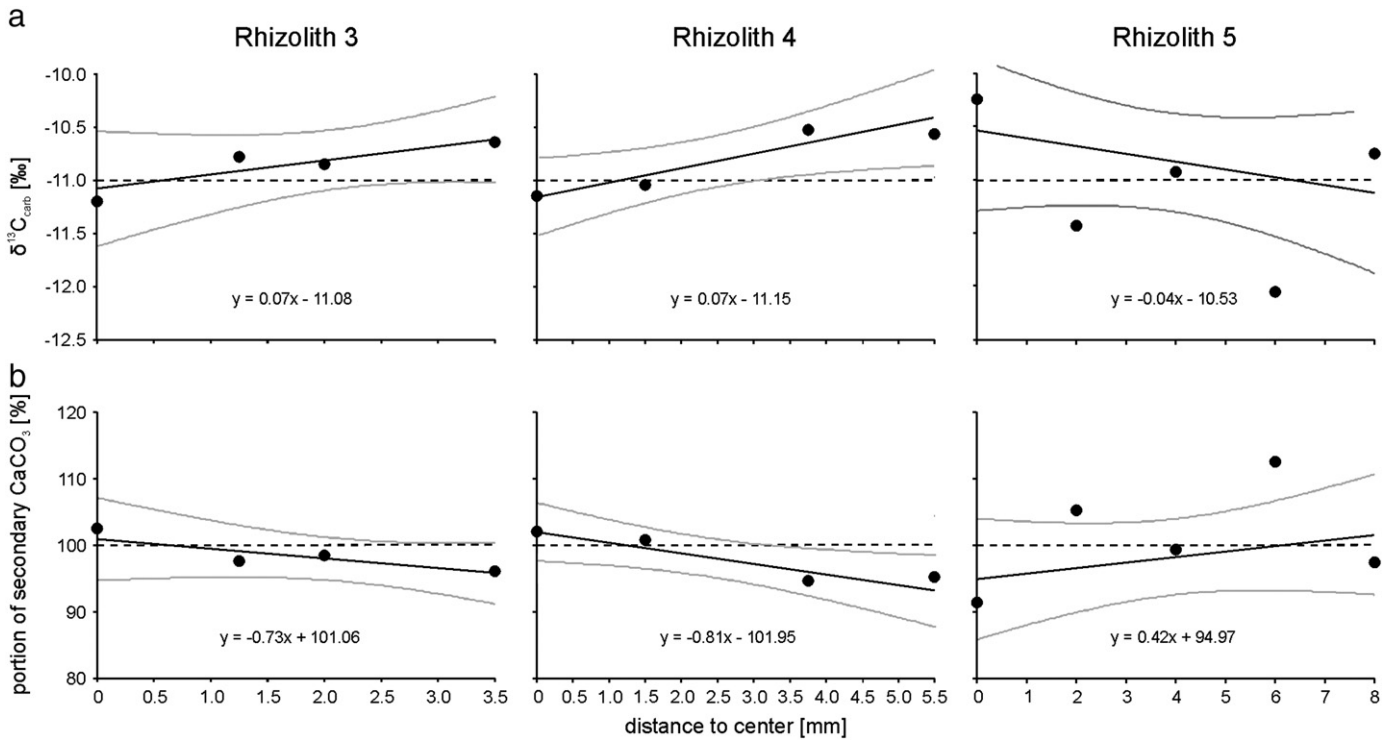
Fig. 5. Microtransects of three rhizolith samples. (a) $\delta^{13}C$ values of rhizolith carbonate, measured in microtransects from the center of the carbonatic tube to the margin; dashed line represents the value of rhizolith $\delta^{13}C_{org} + 14.9‰$ and (b) portions of secondary carbonate in rhizoliths; dashed line represents 100% secondary carbonate. Diameters of rhizolith samples 3, 4 and 5 were 7, 11 and 16 mm, respectively. Diagrams show mean values (black dots) with regression line (black lines) and 95% confidence intervals (gray lines) for each point within the microtransect. For single values of real replicates see electronic supplement. Correlation coefficient r of single values is 0.56, 0.75 and 0.36 for rhizoliths 3, 4 and 5, respectively.

innermost and outermost layers (Pustovoytov et al., 2007b), rhizoliths lack distinct layers (Figs. 1c, 2a–d). Hence, the C_{carb} age of the bulk rhizolith sample is an average age and has to be considered as minimum age for this rhizolith sample from Nussloch. However, in contrast to formation periods of hundreds to thousands of years for secondary carbonate distant from roots (e.g. pseudomycels, loess dolls; Chen and Polach, 1986; Pendall et al., 1994; Kuzyakov et al., 2006), rhizoliths might form within considerably shorter periods, even during the lifetime of the plant and the initial decay of its residues. This is related to the high CO_2 concentration in the rhizosphere and transpirational pull of the plant, leading to preferred Ca^{2+} and HCO_3^- mass flow towards the root (Gocke et al., 2010b).

Radiocarbon ages of rhizolith C_{carb} and C_{org} both were in the same order of magnitude, indicating that rhizolith carbonate was formed in isotopic equilibrium with root- and rhizomicroorganism-derived CO_2 without considerable contamination by introduction of C of other ages. In older secondary carbonates (>tens of thousands of years) even small contamination with modern ^{14}C (<10%) can yield radiocarbon ages that lead to underestimations in the range of thousands of years (Deutz et al., 2002). In contrast, theoretical incorporation of 10% of modern ^{14}C in the rather young Nussloch rhizolith would reduce its true carbonate age only by 470 years. However, the slightly higher age of the rhizolith carbonate compared to included C_{org} indicates that the rhizolith carbonate was not

appreciably contaminated with younger C. This lack of postsegregational alteration was also confirmed by the slightly increasing $\delta^{13}C_{carb}$ values towards the outer parts of rhizoliths (Fig. 5a), which is probably related to the incorporation of primary carbonate grains (Fig. 2a, d).

Assuming that the root was encrusted by secondary carbonate during its lifetime within a few years to a few decades at maximum, the difference between ages of the rhizolith carbonate and enclosed OM ($\Delta \approx 640$ years) probably results from the occlusion of a minor portion of primary carbonate from loess. Previously, this has been referred to as 'limestone dilution effect' (Williams and Polach, 1971). However, it appears more likely that in secondary carbonate this results from mechanical admixtures of lithogenic carbonate (Amundson et al., 1989; Monger et al., 1998) or by microbial decomposition of ^{14}C-depleted OM (Wang et al., 1994). Based on calibrated radiocarbon ages of the rhizolith sample, and assuming an age of the surrounding loess carbonate of >70 000 years (the upper limit for radiocarbon dating), the portion of occluded old carbonate in the radiocarbon dated rhizolith sample was 7.4%.

Mainly, two factors are known that may inhibit carbonate alteration by postsegregational processes (Chen and Polach, 1986; Amundson et al., 1994): dry climatic conditions and high density of the carbonate material. Climatic reasons can be ruled out in the humid region of Nussloch (Heidelberg: 804 mm mean annual precipitation, www.klimadiagramme.de, accessed 02.12.10). Rhizoliths showed high carbonate contents around 85% and at the same time considerable porosities between 15 and 35% (Fig. 2a–d), which is higher than porosity of micritic nodules (Khormali et al., 2006; Pietsch and Kühn, 2009). We suggest that high carbonate contents and compactness of the investigated rhizoliths together with good drainage properties of loess might have led to conservation of the rhizolith carbonate. Moreover, after decay of the roots, the CO_2 concentration decreased very fast in the vicinity of the former root,

Table 1
Radiocarbon ages of C_{carb} and C_{org} in a rhizolith sampled 1.3 m below the present soil surface from the loess–paleosol sequence at Nussloch.

Sample material	^{14}C age, uncal. [years BP]	^{14}C age, cal. (1σ range) [years BP]	^{14}C age, cal., mean ± 1σ [years BP]
Rhizolith C_{carb}	3510 ± 45	3729–3847	3788 ± 59
Rhizolith C_{org}	2969 ± 34	3091–3209	3150 ± 59

and without high CO_2 concentration and water uptake by roots, no further carbonate movement and recrystallization occurred around the rhizoliths (Hinsinger, 1998). This circumstance also supports the suggestion that rhizoliths are formed during the lifetime of plant roots and not after decay of the root tissue, as assumed by other authors (e.g. Joseph and Thrivikramaji, 2006).

4.3. Implications for rhizolith formation in loess

According to the model of Cerling (1984, 1999), the portion of primary carbonate should be almost zero in all secondary carbonates, because CO_2 fluxes from root respiration are 2–3 orders of magnitude higher than rates of carbonate accumulation. This leads to complete replacement of primary C_{carb} with root-respired C during several cycles of carbonate dissolution and reprecipitation. Cerling (1999) and Monger et al. (1998), however, mentioned that primary carbonate can be occluded in secondary carbonates either in a mechanical or chemical way, thereby leading to wrong interpretation of the carbon isotopic signature of secondary carbonates.

So far, it is still under debate whether a complete C_{carb} exchange had happened during rhizolith formation. Due to adjacency to the rhizosphere, this special form of secondary carbonate might be formed in much shorter periods (years to decades; Gocke et al., 2010b) than non-concretional secondary carbonates (hundreds to thousands of years; Kuzyakov et al., 2006; Gocke et al., 2010b). If primary carbonate is present in the parent material (e.g. loess) to a large extent, fast precipitation of secondary carbonate might lead to incomplete dissolution of primary carbonate material. Thus inherited detrital carbonate in secondary carbonate concretions can yield too old radiocarbon ages of the secondary carbonate. Moreover, loess commonly contains primary carbonate not only as $CaCO_3$, but also as dolomite ($CaMg[CO_3]_2$) which can comprise up to ~10% of loess weight (Pye and Sherwin, 1999). During dissolution of primary loess carbonate and reprecipitation of secondary rhizolith carbonate around the roots, lower solubility of dolomite compared to calcite might have led to occlusion of dolomite grains, resulting in a slight overestimation of the age of the rhizolith carbonate. This suggestion is supported by the slightly higher radiocarbon age of rhizolith C_{carb} when compared to rhizolith C_{org}, as well as the occurrence of primary mineral grains (also $CaCO_3$) mainly in the outer part of the rhizoliths (Fig. 2a, d).

Rhizoliths of one horizon can have different ages, thus ruling out general conclusions about the age of rhizolith formation (Ziehen, 1980). Pustovoytov and Terhorst (2004) showed for a loess profile near Nussloch that calcified root cells in upper horizons can be older than those obtained from deeper horizons (9 ky in 0.6 m versus 6 ky in 3 m). Isotopic signatures in our study suggest the absence of contamination of rhizolith carbonate by postsegregational incorporation of C of younger age. This means also that sparite, a feature of recrystallization that occurs in the rhizoliths (Fig. 2e), cannot be much younger than the surrounding micritic carbonate. Radiocarbon ages of the calcified roots in the region south of Heidelberg (Pustovoytov and Terhorst, 2004; this study) provide correct chronologic information about the time of their formation. So far, only three ^{14}C ages for calcified roots are available for the region of SW Germany, all of them indicating Holocene age. As the data base is very low and the three ^{14}C ages coincide with different stratigraphical units, general conclusions regarding the climatic conditions promoting rhizolith formation in loess are not possible. Nevertheless, we speculate here that root calcification occurs mainly during periods of rather dry climatic conditions and/or moisture regimes with strong seasonality. For a rhizolith sample from South African dune sands, Cramer and Hawkins (2009) reported a carbonate ^{14}C age of 7.7 ka. The authors concluded that the rhizolith was formed either during a warm, dry period (the 'Holocene altithermal') or shortly before the onset of this period.

Further investigations are required to allow for statements about climatic drivers forcing the formation of rhizoliths.

4.4. Implications of the rhizolith–loess macrotransects

C_{carb} as well as C_{org} contents were considerably larger in rhizoliths than in loess, which was shown by both the secondary nature of rhizolith carbonate and the comparatively good preservation of rhizolith OM due to encrustation by carbonate.

Living roots can generate remarkable amounts of exudates, and decaying root biomass can lead to a notable input of OM in soil or sediment (Kuzyakov and Domanski, 2000; Nguyen, 2003). Due to a large abundance of rhizoliths in the Nussloch loess section (app. 10–20 rhizoliths m^{-2}) it can be stated that rhizodeposits contributed a considerable portion of postsedimentary OM in the loess. Differentiation between rhizosphere loess and reference loess was, however, not possible based on C_{org} and C_{carb} contents (Fig. 3a).

Portions of secondary carbonate, calculated from $\delta^{13}C_{carb}$, indicated that pedogenic processes were also effective in loess distant to visible root remains. However, these values are not suitable to quantify the input of root-derived OM in rhizosphere loess. Based on lipid analyses, Gocke et al. (2010a) showed that microbial degradation of OM was stronger in rhizosphere loess when compared to rhizoliths and reference loess which was attributed to stronger microbial activity in this former rhizosphere due to exudates and root fragments. As degradation leads to ^{13}C enrichment in C_3 roots (Wiesenberg et al., 2004), highest $\delta^{13}C_{org}$ values should occur in rhizosphere loess when compared to rhizoliths and loess. This trend was visible only in one of the macrotransects (rhizolith 1; Fig. 3b), however without significant differences. Very likely, changes of $\delta^{13}C_{org}$ values in rhizosphere loess, caused by addition of unknown portions of stronger microbially degraded OM to the original synsedimentary OM, are too small to be detected by isotope ratio mass spectrometry, which can also be related to sample heterogeneity. Thus, these $\delta^{13}C_{org}$ values, too, can neither be used to differentiate between loess adjacent to roots and root-free loess, nor to determine the amount of root biomass that was incorporated postsedimentary. Furthermore, the variability of $\delta^{13}C_{org}$ values of rhizoloess in horizontal transects (>1‰) leads to the question, how meaningful low differences in loess $\delta^{13}C_{org}$ values within a vertical transect (<1‰) of the sedimentary sequence are (Hatté et al., 1999). Lipid analyses of rhizolith and loess OM provide a tool for the elucidation of these uncertainties: Based on two different lipid molecular proxies, Gocke et al. (2010a) demonstrated the incorporation of considerable amounts of root-derived OM in loess adjacent to rhizoliths: 111% and 70% in rhizosphere loess 1 (0–2.5 cm) and 11% and 5% in rhizosphere loess 2 (2.5–5 cm).

4.5. Chronologic implications for paleoenvironmental reconstructions

In the region south of Heidelberg, maximum ages of 9 ka for rhizoliths and calcified root cells show that they formed in the Holocene (Pustovoytov and Terhorst, 2004; this study), while surrounding loess was deposited mainly during the last glacial–interglacial cycle (Zöller et al., 1988; Hatté et al., 1998). At Nussloch, rhizoliths from a depth of 1.3 m are considerably younger with 3 ka when compared to surrounding loess which was deposited between 17 ka and 20 ka before present (Antoine et al., 2001).

For terrestrial paleoclimate archives other than loess it has been recognized that properties of the original, synsedimentary OM may have been altered by introduction of younger roots. For a Chinese peat sequence, Zhou et al. (2005) calculated a contamination of up to 16% of modern C caused by postsedimentary incorporation of younger plant biomass. Similar conditions can occur in loess–paleosol sequences (Head et al., 1989). Liu et al. (2007) suggest an older source for the contamination of the synsedimentary plant signal in

loess: OM of the source material of loess. Our current results (this study; Gocke et al., 2010a), however, suggest that an admixture of younger, i.e. postsedimentary OM is more likely. This can entail serious problems concerning the reliability of ^{14}C ages of loess OM (Hatté et al., 1998; Rousseau et al., 2007). Consequences for bulk $\delta^{13}C_{org}$ might be negligible, if both the synsedimentary and the younger organic materials derived from C_3 vegetation, and if the only purpose of $\delta^{13}C_{org}$ measurement is the determination of the photosynthetic pathway of vegetation. However, reconstruction of paleoprecipitation from loess $\delta^{13}C_{org}$ (Hatté and Guiot, 2005), based on small variations of $\delta^{13}C$ values, might be disturbed by postsedimentary input of root-derived C_{org}, which is not necessarily uniform throughout complete loess–paleosol sequences.

Considerable age discrepancies (>10 ka) are possible also between secondary carbonate and surrounding loess (Pustovoytov and Terhorst, 2004; this study). This problem might be important also for other loess–paleosol sequences. It was not perceived by Wang et al. (2000), who studied secondary carbonates in loess–paleosol sequences on the Chinese Loess Plateau and in central North America. The authors reported a considerably wider spectrum for the difference between stable carbon isotopic composition of secondary carbonate and of OM from surrounding loess than the difference of ~15‰ suggested by Nordt et al. (1996). These differences in $\delta^{13}C$ values were linked to monsoonal and paleo-El Niño variations, whereas the true reason may be the different source vegetation of secondary carbonate and loess OM.

It is still a prevalent belief that total OM and secondary carbonate formed synsedimentary in loess (e.g. Becze-Deák et al., 1997; Wang et al., 2000, 2004). So far, only few studies mentioned the possibility that secondary carbonate formation in loess–paleosol sequences might have occurred later than sedimentation, however without testing this idea by comparison of radiocarbon ages of rhizoliths and synsedimentary loess C_{org} (Boguckyj et al., 2009). The presumption was confirmed by first radiocarbon data from calcified roots from loess–paleosol sequences (Pustovoytov and Terhorst, 2004; Cramer and Hawkins, 2009; this study). Whereas in the present study, C_{org} contents were similar in loess distant and adjacent to rhizoliths, it was also possible to elucidate differences in the molecular composition of the OM therein as determined for lipid content and lipid composition between rhizoloess and reference loess (Gocke et al., 2010a). It was observed that remarkable amounts of root-derived OM were incorporated in loess at least up to a distance of 5 cm from rhizoliths and possibly even in larger distances. Together with the fact that rhizoliths were formed later and by a different vegetation than loess OM, this might entail uncertainties for bulk analyses in loess OM, as e.g. $\delta^{13}C_{org}$ and radiocarbon dating.

5. Conclusions

Based on elemental and isotopic C analyses on organic and carbonatic compounds of loess and rhizoliths (calcified roots) from the loess–paleosol sequence at Nussloch, SW Germany, we conclude that

- rhizoliths were formed by C_3 vegetation;
- during formation of the rhizoliths, C from primary loess carbonate was almost completely exchanged with C from CO_2 respired by roots and rhizosphere microorganisms, leading to portions of secondary carbonate of nearly 100% as derived from $\delta^{13}C$ data;
- rhizoliths were generated fast: during the lifetime of the roots as obtained from radiocarbon data;
- the largest part of the carbonate material of the rhizoliths was not recrystallized postsegregationally, justifying their suitability for radiocarbon dating;
- rhizoliths are considerably younger than surrounding loess ($\Delta \approx 14$ ka at minimum) (^{14}C, luminescence dating); and

- postsedimentary root penetration into loess probably led to an overprint of the original signal of loess OM, which, however, cannot be estimated by means of C_{org} contents or stable carbon isotopic composition.

Appendix A. Supplementary data

Supplementary data to this article can be found online at doi:10.1016/j.chemgeo.2011.01.022.

References

Alonso-Zarza, A.M., 1999. Initial stages of laminar calcrete formation by roots: examples from the Neogene of central Spain. Sedimentary Geology 126, 177–191.

Amundson, R., Chadwick, O., Sowers, J., Doner, H., 1989. The stable isotope chemistry of pedogenic carbonates at Kyle Canyon, Nevada. Soil Science Society of America Journal 53, 201–210.

Amundson, R., Wang, Y., Chadwick, O.A., Trumbore, S.E., McFadden, L., McDonald, E., Wells, S., DeNiro, M., 1994. Factors and processes governing the ^{14}C content of carbonate in desert soils. Earth and Planetary Science Letters 125, 385–405.

Antoine, P., Rousseau, D., Zöller, L., Lang, A., Munaut, A.V., Hatté, C., Fontugne, M., 2001. High-resolution record of the last interglacial–glacial cycle in the Nussloch loess–palaeosol sequences, Upper Rhine Area, Germany. Quaternary International 76 (77), 211–229.

Antoine, P., Rousseau, D., Moine, O., Kunesch, S., Hatté, C., Lang, A., Tissoux, H., Zöller, L., 2009. Rapid and cyclic aeolian deposition during the Last Glacial in European loess: a high-resolution record from Nussloch, Germany. Quaternary Science Reviews 28, 2955–2973.

Asano, M., Tamura, K., Maejima, Y., Matsuzaki, H., Higashi, T., 2007. $\Delta^{14}C$ variations of pedogenic carbonate in Mongolian steppe soils under a vegetation sequence. Nuclear Instruments and Methods in Physics Research B 259, 403–407.

Beckmann, T., 1997. Präparation bodenkundlicher Dünnschliffe für mikromorphologische Untersuchungen. Hohenheimer Bodenkundliche Hefte 40, 89–103.

Becze-Deák, J., Langohr, R., Verrecchia, E., 1997. Small scale secondary $CaCO_3$ accumulations in selected sections of the European loess belt: morphological forms and potential for paleoenvironmental reconstruction. Geoderma 76, 221–252.

Bente, B., Löscher, M., 1987. Sedimentologische, pedologische und stratigraphische Untersuchungen an Lössen südlich Heidelberg. Göttinger Geographische Abhandlungen 84, 9–17.

Boguckyj, A.B., Łanczont, M., Łącka, B., Madeyska, T., Sytnyk, O., 2009. Age and the palaeoenvironment of the West Ukrainian palaeolithic: the case of Velykyi Glybochok multi-cultural site. Journal of Archaeological Science 36, 1376–1389.

Buck, B.J., Monger, H.C., 1999. Stable isotopes and soil-geomorphology as indicators of Holocene climate change, northern Chihuahuan Desert. Journal of Arid Environments 43, 357–373.

Budd, D.A., Pack, S.M., Fogel, M.L., 2002. The destruction of paleoclimatic isotopic signals in Pleistocene carbonate soil nodules of Western Australia. Palaeogeography, Palaeoclimatology, Palaeoecology 188, 249–273.

Cerling, T.E., 1984. The stable isotopic composition of modern soil carbonate and its relation to climate. Earth and Planetary Science Letters 71, 229–240.

Cerling, T.E., 1999. Stable carbon isotopes in paleosol carbonates. In: Thiry, M., Simon-Coinçon, R. (Eds.), Palaeoweathering, Palaeosurfaces, and Related Continental Deposits. Cambridge, Blackwells, pp. 43–60.

Chen, Y., Polach, H., 1986. Validity of ^{14}C ages of carbonate in sediments. Radiocarbon 28, 464–472.

Cramer, M.D., Hawkins, H.J., 2009. A physiological mechanism for the formation of root casts. Palaeogeography, Palaeoclimatology, Palaeoecology 274, 125–133.

Deines, P., 1980. The isotopic composition of reduced organic compounds. In: Fritz, P., Fontes, J.C. (Eds.), Handbook of Environmental Isotope Geochemistry. Amsterdam, Elsevier, pp. 329–406.

Deutz, P., Montanez, I.P., Monger, H.C., 2002. Morphology and stable and radiogenic isotope composition of pedogenic carbonates in late Quaternary relict soils, New Mexico, U.S.A.: an integrated record of pedogenic overprinting. Journal of Sedimentary Research 72, 809–822.

Dultz, S., Kühn, P., 2005. Occurrence, formation, and micromorphology of gypsum in soils from the Central-German Chernozem region. Geoderma 129, 230–250.

Gocke, M., Wiesenberg, G.L.B., Pustovoytov, K., Kuzyakov, Y., 2010a. Rhizoliths in loess — evidence for post-sedimentary incorporation of root-derived organic matter in terrestrial sediments as assessed from molecular proxies. Organic Geochemistry 41, 1198–1206.

Gocke, M., Pustovoytov, K., Kuzyakov, Y., 2010b. Carbonate recrystallization in root-free soil and rhizosphere of *Triticum aestivum* and *Lolium perenne* estimated by ^{14}C labeling. Biogeochemistry. doi:10.1007/s10533-010-9456-z.

Hatté, C., Guiot, J., 2005. Palaeoprecipitation reconstruction by inverse modelling using the isotopic signal of loess organic matter: application to the Nußloch loess sequence (Rhine Valley, Germany). Climate Dynamics 25, 315–327.

Hatté, C., Fontugne, M., Rousseau, D., Antoine, P., Zöller, L., Tisnerat-Laborde, N., Bentaleb, I., 1998. δ^{13}C variations of loess organic matter as a record of the vegetation response to climatic changes during the Weichselian. Geology 26, 583–586.

Hatté, C., Antoine, P., Fontugne, M., Rousseau, D., Tisnerat-Laborde, N., Zöller, L., 1999. New chronology and organic matter δ^{13}C paleoclimatic significance of Nußloch loess sequence (Rhine Valley, Germany). Quaternary International 62, 85–91.

Head, M.J., Zhou, W.J., Zhou, M.F., 1989. Evaluation of ^{14}C ages of organic fractions of paleosols from loess–paleosol sequences near Xian, China. Radiocarbon 31, 680–694.

Hinsinger, P., 1998. How do plant roots acquire mineral nutrients? Chemical processes involved in the rhizosphere. Advances in Agronomy 64, 225–265.

Hinsinger, P., Plassard, C., Tang, C., Jaillard, B., 2003. Origins of root-mediated pH changes in the rhizosphere and their responses to environmental constraints: a review. Plant and Soil 248, 43–59.

Jaillard, B., 1992. Calcification des cellules corticales des racines en milieu calcaire. Bulletin de la Société de Botanique de France 139, 41–46.

Jaillard, B., Guyon, A., Maurin, A.F., 1991. Structure and composition of calcified roots, and their identification in calcareous soils. Geoderma 50, 197–210.

Joseph, S., Thrivikramaji, K.P., 2006. Rhizolithic calcrete in Teris, southern Tamil Nadu: origin and paleoenvironmental implications. Journal of the Geological Society of India 65, 158–168.

Kadereit, A., Kühn, P., Wagner, G., 2010. Holocene relief and soil changes in loess-covered areas of south-western Germany − the pedosedimentary archives of Bretten-Bauerbach (Kraichgau). Quaternary International 222, 96–119.

Kemp, R.A., Derbyshir, E., Xingmi, M., Fah, C., Baotia, P., 1994. Pedosedimentary reconstruction of a thick loess–paleosol sequence near Lanzhou in North-Central China. Quaternary Research 43, 30–45.

Khokhlova, O.S., Kovalevskaya, I.S., Oleynik, S.A., 2001. Records of climatic changes in the carbonate profiles of Russian Chernozems. Catena 43, 203–215.

Khormali, F., Abtahi, A., Stoops, G., 2006. Micromorphology of calcitic features in highly calcareous soils of Fars Province, Southern Iran. Geoderma 132, 31–46.

Klappa, C.F., 1980. Rhizoliths in terrestrial carbonates: classification, recognition, genesis and significance. Sedimentology 27, 613–629.

Kosir, A., 2004. Microcodium revisited: root calcification products of terrestrial plants on carbonate-rich substrates. Journal of Sedimentary Research 74, 845–857.

Kuzyakov, Y., Domanski, G., 2000. Carbon input by plants into the soil. Review. Journal of Plant Nutrition and Soil Science 163, 421–431.

Kuzyakov, Y., Shevtzova, E., Pustovoytov, K., 2006. Carbonate re-crystallization in soil revealed by ^{14}C labeling: experiment, model and significance for paleo-environmental reconstructions. Geoderma 131, 45–58.

Łącka, B., Łanczont, M., Madeyska, T., 2009. Oxygen and carbon stable isotope composition of authigenic carbonates in loess sequences from the Carpathian margin and Podolia, as a palaeoclimatic record. Quaternary International 198, 136–151.

Liu, W., Yang, H., Ning, Y., An, Z., 2007. Contribution of inherent organic carbon to the bulk δ^{13}C signal in loess deposits from the arid western Chinese Loess Plateau. Organic Geochemistry 38, 1571–1579.

Löscher, M., Haag, T., 1989. Zum Alter der Dünen im nördlichen Oberrheingraben bei Heidelberg und zur Genese ihrer Bänderparabraunerden. Eiszeitalter und Gegenwart 39, 98–108.

Mason, J.A., Miao, X., Hanson, P.R., Johnson, W.C., Jacobs, P.M., Goble, R.J., 2008. Loess record of the Pleistocene–Holocene transition on the northern and central Great Plains, USA. Quaternary Science Reviews 27, 1772–1783.

Monger, H.C., Cole, D.R., Gish, J.W., Giordano, T.H., 1998. Stable carbon and oxygen isotopes in Quaternary soil carbonates as indicators of ecogeomorphic changes in the northern Chihuahuan Desert, USA. Geoderma 82, 137–172.

Mora, C.I., Driese, S.G., Colarusso, L.A., 1996. Middle to late Paleozoic atmospheric CO_2 levels from soil carbonate and organic matter. Science 271, 1105–1107.

Nguyen, C., 2003. Rhizodeposition of organic C by plants: mechanisms and controls. Agronomie 23, 375–396.

Nordt, L., Wilding, L., Hallmark, C., Jacob, J., 1996. Stable carbon isotope composition of pedogenic carbonates and their use in studying pedogenesis. In: Boutton, T.W.,

Yamasaki, S. (Eds.), Mass Spectrometry of Soils. Marcel Dekker, New York, pp. 133–154.

Nordt, L., Hallmark, C., Wilding, L., Boutton, T., 1998. Quantifying pedogenic carbonate accumulations using stable carbon isotopes. Geoderma 82, 115–136.

O'Leary, M.H., 1981. Carbon isotope fractionation in plants. Phytochemistry 20, 553–567.

Pendall, E., Harden, J., Trumbore, S., Chadwick, O., 1994. Isotopic approach to soil carbonate dynamics and implications for paleoclimatic interpretations. Quaternary Research 42, 60–71.

Pietsch, D., Kühn, P., 2009. Soil development stages of layered Cambisols and Calcisols on Socotra Island, Yemen. Soil Science 174, 292–302.

Pustovoytov, K., Terhorst, B., 2004. An isotopic study of a late Quaternary loess–paleosol sequence in SW Germany. Revista Mexicana de Ciencias Geologicas 21, 88–93.

Pustovoytov, K., Schmidt, K., Taubald, H., 2007a. Evidence for Holocene environmental changes in the northern Fertile Crescent provided by pedogenic carbonate coatings. Quaternary Research 67, 315–327.

Pustovoytov, K., Schmidt, K., Parzinger, H., 2007b. Radiocarbon dating of thin pedogenic carbonate laminae from Holocene archaeological sites. The Holocene 17, 835–843.

Pye, K., Sherwin, D., 1999. Loess. Ch. 10. In: Goudie, A.S., Livingstone, I., Stokes, S. (Eds.), Aeolian Environments, Sediments and Landforms. Wiley, Chichester, pp. 213–238.

Quade, J., Cerling, T.E., 1995. Expansion of C$_4$ grasses in the Late Miocene of Northern Pakistan: evidence from stable isotopes in paleosols. Palaeogeography, Palaeoclimatology, Palaeoecology 115, 91–116.

Roberts, H.M., 2008. The development and application of luminescence dating to loess deposits: a perspective on the past, present, and future. Boreas 37, 483–507.

Romanek, C.S., Grossman, E.L., Morse, J.W., 1992. Carbon isotopic fractionation in synthetic aragonite and calcite: effects of temperature and precipitation rate. Geochimica and Cosmochimica Acta 56, 419–430.

Rousseau, D.D., Sima, A., Antoine, P., Hatté, C., Lang, A., Zöller, L., 2007. Link between European and North Atlantic abrupt climate changes over the last glaciation. Geophysical Research letters 34, L22713.

Stoops, G., 1976. On the nature of "lublinite" from Hollanta (Turkey). American Mineralogist 61, 172.

Stoops, G., 2003. Guidelines for Analysis and Description of Soil and Regolith Thin Sections. Soil Science Society of America, Madison, Wisconsin. 184 pp.

Wang, H., Greenberg, S.E., 2007. Reconstructing the response of C$_3$ and C$_4$ plants to decadal-scale climate change during the late Pleistocene in southern Illinois using isotopic analyses of calcified rootlets. Quaternary Research 67, 136–142.

Wang, Y., Amundson, R., Trumbore, S., 1994. A model for soil [14]CO_2 and its implications for using ^{14}C to date pedogenic carbonate. Geochimica et Cosmochimica Acta 58, 393–399.

Wang, H., Follmer, L.R., Liu, J.C.-I., 2000. Isotope evidence of paleo–El Nino–Southern Oscillation cycles in loess–paleosol record in the central United States. Geology 28, 771–774.

Wang, H., Ambrose, S.H., Fouke, B.W., 2004. Evidence of long-term seasonal climate forcing in rhizolith isotopes during the last glaciation. Geophysical Research Letters 31, L13203.

Weninger, B., Jöris, O., Danzeglocke, U., 2007. CalPal-2007. Cologne radiocarbon calibration and palaeoclimate research package. http://www.calpal.de/2007 (accessed 24.02.10).

Wiesenberg, G.L.B., Schwarzbauer, J., Schmidt, M.W.I., Schwark, L., 2004. Source and turnover of organic matter in agricultural soils derived from n-alkane/n-carboxylic acid compositions and C-isotope signatures. Organic Geochemistry 35, 1371–1393.

Wiesenberg, G.L.B., Gocke, M., Kuzyakov, Y., 2010. Optimization of ^{14}C liquid scintillation counting of plant and soil lipids to trace short term formation, translocation and degradation of lipids. Journal of Radioanalytical and Nuclear Chemistry 284, 99–108.

Williams, G.E., Polach, H.A., 1971. Radiocarbon dating of arid-zone calcareous paleosols. Geological Society of America Bulletin 82, 3069–3086.

Xiao, J., Porter, S.C., Zhisheng, A., Kumai, H., Yoshikawa, S., 1995. Grain size of quartz as an indicator of winter monsoon strength on the Loess Plateau of Central China during the last 130 000 yr. Quaternary Research 43, 22–29.

Zhou, W., Xie, S., Meyers, P.A., Zheng, Y., 2005. Reconstruction of late glacial and Holocene climate evolution in southern China from geolipids and pollen in the Dingnan peat sequence. Organic Geochemistry 36, 1272–1284.

Ziehen, W., 1980. Forschung über Osteokollen I. Mainzer Naturwissenschaftliches Archiv, 18, pp. 1–70.

Zöller, L., Stremme, H., Wagner, G.A., 1988. Thermolumineszenz-Datierung an Löss-Paläoboden-Sequenzen von Nieder-, Mittel und Oberrhein. Chemical Geology (Isotope Geoscience Section) 73, 39–62.